CAPACITIVELY TRANSDUCED MICROMECHANICAL RESONATORS WITH SIMULTANEOUS LOW MOTIONAL RESISTANCE AND $Q > 70,000$

Mehmet Akgul [*], *Bongsang Kim, Zeying Ren and Clark T.-C. Nguyen*
Department of Electrical Engineering and Computer Science
University of California at Berkeley, CA 94720, U.S.A

ABSTRACT

Capacitively transduced micromechanical disk resonators that exhibit simultaneous low motional resistance ($< 130\ \Omega$) and high Q ($>70,000$) at 61 MHz are demonstrated using an improved ALD-partial electrode-to-resonator gap filling technique that reduces the Q-limiting surface losses of previous renditions by adding an alumina pre-coating before ALD of the gap-filling high-k dielectric. This work increases the Q over the ~10,000 of previous renditions by more than 6× towards demonstration of the first VHF micromechanical resonators in any material, piezoelectric or not, to meet the simultaneous high Q ($>50,000$) and low motional resistance R_x ($< 200\Omega$) specs highly desired for front-end frequency channelizer requirements in cognitive and software-defined radio architectures. This work finally overcomes the high impedance bottleneck that has plagued capacitively transduced micromechanical resonators over the past decade.

INTRODUCTION

Capacitively transduced micromechanical resonators have historically achieved the highest Q's among micro-scale counterparts using other technologies [1][2][3], reaching Q's past 200,000 at VHF and 14,600 at 1.2 GHz [4]. Such Q's are highly desired for a myriad of applications, from very narrow band low insertion loss filters for co-site interference suppression [5]; to low phase noise, low power oscillators for radar and communications [6]; to frequency gating spectrum analyzer functions for true software-defined cognitive radio [5]. Additional advantages, like zero DC power consumption and the ability to self-switch, further bolster the argument for using these devices [7].

Still, adaptation of capacitive micromechanical resonators in these applications has so far been slowed by their higher than conventional impedances, which makes them difficult to interface with widely used 50Ω RF components. Theoretically, there is actually no good reason why the impedances of such resonators must be high. In particular, just a quick glance at Eq. (1) governing the motional resistance R_x of the disk array-composite resonator shown

$$R_x = \frac{1}{N}\frac{d_{gap}^4}{V_P^2}\frac{1}{A^2\epsilon_o^2}\frac{\omega_o\, m_{re}}{Q} \quad (1)$$
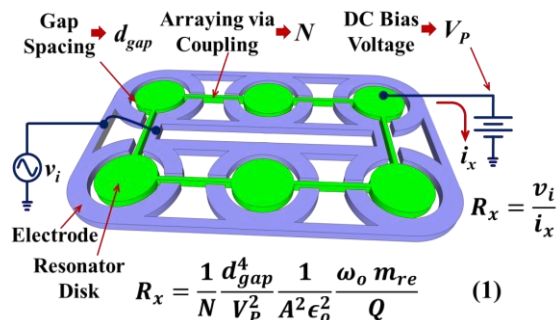
m_{re} : Equivalent dynamic mass Q : Resonator quality factor
ω_o : Resonance frequency in radians ϵ_o : Permittivity of vacuum
A : Overlap area between the electrode and resonator

Fig. 1: Schematic of an array-composite disk resonator, showing a one-port excitation/readout scheme, identifying important variables, and providing the expression for the effective motional resistance R_x of the device.
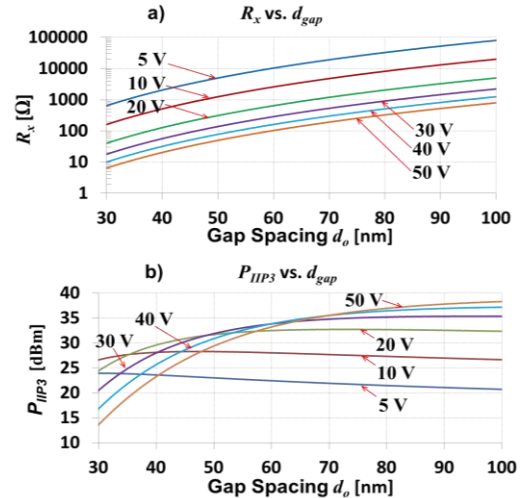
Fig. 2: Simulated plots of (a) motional resistance and (b) IIP_3 versus dc-bias voltage and electrode-to-resonator gap spacing for a 61-MHz wineglass disk resonator with $Q = 70,000$.

in Fig. 1 reveals that there are many knobs to turn that allow a designer to achieve a very wide range of motional resistances. Fig. 2(a) presents curves of R_x versus gap spacing and dc-bias that illustrate the wide range of values attainable by capacitively transduced resonators. Although all the variables in (1) can (and have been) used as knobs to tailor R_x, the 4th power dependence on electrode-to-resonator gap spacing d_{gap} makes it the most effective of the bunch [8]. Furthermore, as detailed in [8], reducing gap spacing is the most effective knob by which to maximize the $\omega_{FOM} = 1/(R_Q C_o)$ figure of merit that governs the efficacy of a given resonator for filter construction. And contrary to popular belief, shrinking d_{gap} does not necessarily reduce resonator linearity, as clearly shown by the IIP_3 versus gap spacing and dc-bias curves of Fig. 2(b), generated using the theory of [9]. Here, for a dc-bias voltage of 20V, the IIP_3 remains above 25 dBm at a gap spacing of 30 nm. For lower dc-bias voltages, e.g., 5V, the IIP_3 remains high for gap spacings well below 30 nm.

Of the approaches to reducing gap spacing towards lower impedance [8][10][11], the partial atomic layer deposition (ALD)-filled gap spacing method described in [8] combines the advantages of better yield relative to brute force gap-release approaches [10][12], and demonstrated application to a lateral disk resonator, to which the silicide gap method of [11] has not yet been applied. Unfortunately, the work of [8] lowered the Q of resonator devices from starting values over 150,000 without partial ALD-gap filling down to only ~10,000 with ALD, supposedly due to surface losses introduced by the HfO$_2$ high-k dielectric film used to partially fill the gap and coat the resonator.

Pursuant to restoring Q's to over 50,000 while simultaneously achieving impedances less than 200Ω, this work employs an alumina (Al$_2$O$_3$) pre-coating layer to improve the material quality of partial gap-filling ALD dielectric material, thereby greatly reducing surface losses towards a more than 6× increase in Q. The measured simultaneous Q of 73,173 and motional resistance of
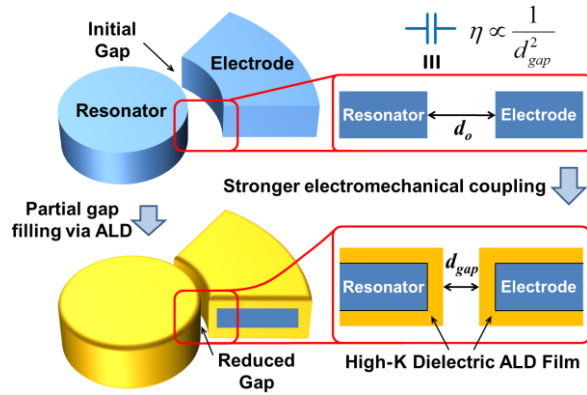
Fig. 3: Schematics summarizing the partial gap-filling gap reduction method of [8], where ALD of a high-k dielectric film effectively reduces the gap distance between the electrode and the disk.

130Ω achieved by this work at 61 MHz further bolster the notion that there are very few limits to the impedance-Q combinations achievable by capacitively transduced micromechanical resonators.

PARTIAL ALD ELECTRODE-TO-RESONATOR GAP FILLING

Partial ALD gap-filling, first demonstrated in [8], comprises a clever way to achieve tiny sub-30nm electrode-to-resonator gaps without the need to etch tiny sacrificial spacer layers, and thus, without the associated yield losses. As described in Fig. 3, the method involves first fabricating and releasing a micromechanical resonator, e.g., a disk resonator, with relatively wide initial electrode-to-resonator gap-spacings that permit good device yield; then coating the resonator and its electrodes with a conformal high-k dielectric ALD film. If the dielectric constant of the dielectric material is sufficiently high, i.e., if it is a "high-k" material, the effective electrode-to-resonator gap spacing of the coated device will be much smaller than the original spacing, and very close to the physical spacing between the dielectric surfaces, as shown in Fig. 3. Since ALD [13] provides a very uniform and conformal film deposition with <1nm thickness accuracy controlled simply by the number of reaction half cycles used, one can tune the final gap spacing to any desired value very accurately, provided the initial gap spacing is well known. This equates to an ability to achieve virtually any low motional resistance in accordance with (1), while simultaneously improving ω_{FOM} and avoiding the excessive chip area (for arraying) and high bias voltage that would otherwise be needed if large gaps are used.

As mentioned, although the work of [8] successfully reduced the gap spacing of a 61-MHz wineglass mode disk resonator from 94 nm to 32 nm by coating the released resonator with a 30.7 nm HfO$_2$ ALD film, it did so with a penalty amounting to a 20x reduction in resonator Q, from the original uncoated Q of 150,527 to a much lower value of 7,368. Needless to say, if not mitigated in some way, such a reduction in Q renders the described partial-gap filling approach quite ineffectual, since Q's less than 30,000 are not sufficient for the RF channel-selection or low phase noise applications targeted by MEMS-based vibrating resonators [5]. With all other parameters that influence energy loss (e.g., pressure, temperature, device geometry, anchor size) held constant before and after the HfO$_2$ ALD coating, the most probable explanation for the reduction in resonator Q is added surface loss arising from poor HfO$_2$ ALD film quality, and this was indeed postulated in [8].

If surface losses are the main culprit here, then methods for improving ALD film quality are required. Indeed, the need to mitigate surface-film-based loses becomes even more urgent as devices
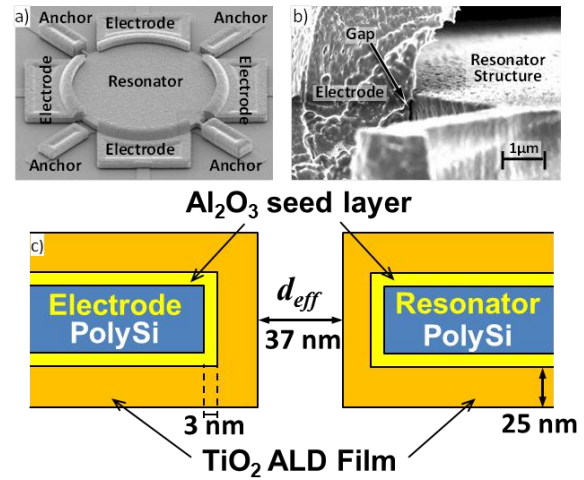

Fig. 4: SEM images of a) a polysilicon micromachined wine-glass mode disk resonator before gap tuning and b) cross-section after conformal ALD of 3nm Al$_2$O$_3$ + 25nm TiO$_2$. c) Schematic showing reduction of the resonator-to-electrode gap size from 87nm to 37nm via ALD partial-gap filling.

are scaled towards higher frequency, since scaling raises the surface-to-volume ratio, making surface-derived loss mechanisms even more prominent.

IMPROVING ALD FILM QUALITY

Pursuant to reducing surface-derived losses, this work attempts to improve the ALD film quality by more properly nucleating the high-k dielectric ALD as it grows. In particular, the key to the order of magnitude Q boost in this work is the introduction of an interfacial 3nm Al$_2$O$_3$ ALD pre-coating before ALD of the much higher-k gap-filling dielectric film—in this case, 25nm of TiO$_2$—shown in Fig. 4(c). The need for such a pre-coating is governed by the ALD deposition chemistry of TiO$_2$, which requires a healthy forest of dangling OH bonds over the starting surface to achieve a conformal and high quality film [14]. Without the pre-coating of Al$_2$O$_3$, the number of free OH bonds on the silicon surface is comparatively sparse, resulting in nucleation problems for the TiO$_2$ film that in turn lead to Q-reducing surface defects and losses (Fig. 5(a)). Al$_2$O$_3$ is an excellent choice for the pre-coating, because it depends less on a perfectly hydroxylated surface; i.e., it
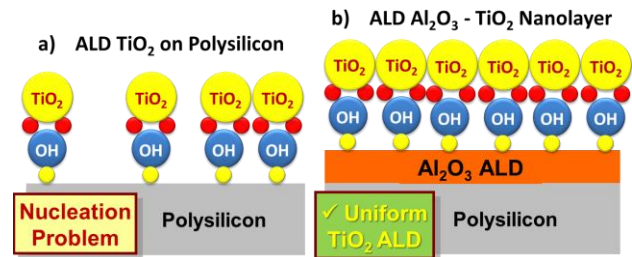

Fig. 5: a) Good quality TiO$_2$ ALD film requires good surface hydroxylation, i.e. a rich and uniform OH (hydroxyl) layer, which silicon lacks, leading to a nucleation problem and resultant surface loss mechanism that reduces the resonator Q. b) Al$_2$O$_3$ grows good quality films on various substrates, even without good hydroxylation, and also provides a dense and uniform forest of AlOH hydroxyl group. This then leads to a uniform subsequent TiO$_2$ ALD, eliminating surface loss mechanisms that otherwise limit the resonator Q.
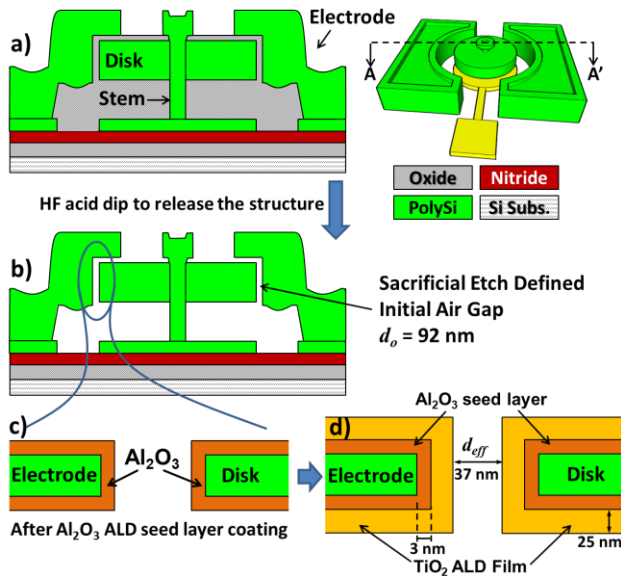
M. Akgul, B. Kim, Z. Ren, and C. T.-C. Nguyen, "Capacitively transduced micromechanical resonators with simultaneous low motional resistance and Q >70,000," *Tech. Digest*, 2008 Solid-State Sensor, Actuator, and Microsystems Workshop, Hilton Head, South Carolina, June 6-10, 2010, pp. 467-470.

Fig. 6: Cross-sections describing the process flow for Al_2O_3–TiO_2 nanolayer ALD partial-gap filling.
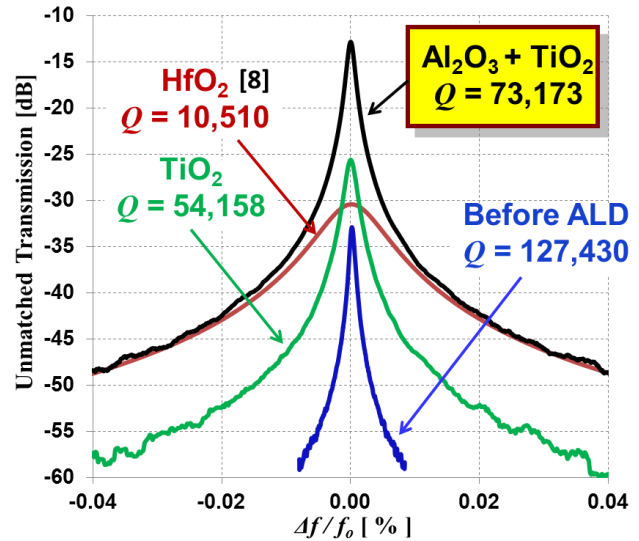

Fig. 7: Comparison of measured frequency characteristics under vacuum with dc-bias voltage of 9V for 61-MHz wine-glass disk resonators treated with various ALD partial gap filling recipes.

ALDs into good quality films on various substrates, including silicon, whether or not the starting OH forest is sparse [15].

Of course, Al_2O_3's dielectric constant (k=9) is too low to serve as the primary gap-filling material, so the thickness of the Al_2O_3 film should be kept small: for this work, on the order of 3 nm. Although very thin, this Al_2O_3 film still provides the desired OH surface for the much higher-k (k=80) TiO_2 film to follow [16], as described in Fig. 5(b). Now, with Al_2O_3 present, the TiO_2 film can be deposited free of nucleation defects, hence, with much better quality and fewer sites for defect-derived energy loss. As a result, this Al_2O_3-TiO_2 bilayer approach achieves an optimal solution that provides simultaneous narrow gaps for low motional resistance and low surface losses for high Q.

ALD PARTIAL GAP FILLING PROCESS FLOW

Fig. 6 summarizes the process flow for the ALD partial gap filling process, with the new measures described above to pre-coat structure surfaces with an Al_2O_3 seed layer prior to ALD of the main partial gap filling high-k dielectric TiO_2. The process starts with conventional steps [17] to achieve an unreleased 61-MHz wineglass mode disk resonator in polysilicon with 87 nm lateral electrode-to-resonator gaps temporarily filled with sacrificial high temperature oxide (HTO), as shown in Fig. 6(a). The resonator is then dipped in a 49% HF acid bath for 30 minutes to etch the sacrificial oxide and release the structure, yielding the cross-section of Fig. 6(b). Because the gaps are 87 nm, and not smaller, the yield of the release etch can be quite high, in excess of ~95%.

Next, the released resonator is coated with a 3nm Al_2O_3 ALD to achieve the cross-section of Fig. 6(c). This Al_2O_3 layer is quite conformal over the polysilicon surface, which is necessary if it is to serve as a seed layer providing a uniform and dense AlOH hydroxylated surface for a subsequent ALD of 25 nm thick TiO_2. Fig. 6(d) presents the final cross-section of the device, for which the final effective gap spacing is 37 nm. For comparative purposes, versions of the process were also run without the Al_2O_3 pre-coating and just ALD'ing 25 nm TiO_2 directly over the polysilicon resonator surfaces.

To allow for electrical connection to bond pads, a final lithography step is performed to cover all released devices and expose their bond pads, after which a very short HF dip removes ALD material over the bondpads. Photoresist is then removed via acetone, and critical point drying applied to clean devices.

EXPERIMENTAL RESULTS

To verify the efficacy of Al_2O_3 pre-coating as a method for reducing surface losses, the frequency characteristics of 61-MHz wine-glass disk resonators treated with various ALD-coating recipes were measured under 1 μTorr vacuum in direct two-port configurations using an HP 5070B network analyzer. All tested devices were identical prior to ALD-coating, and all were measured under the exact same electrical connection and vacuum conditions. Fig. 7 compares measured frequency characteristics for 61-MHz wine-glass disk resonators with electrode-to-resonator gaps partially filled with 25nm of TiO_2 only, without the Al_2O_3 seed layer; and 3nm Al_2O_3+25nm TiO_2; showing Q's of 54,158 and 73,173, respectively, which clearly indicates the benefits of Al_2O_3 pre-coating. Comparison of these results with data from [8] (included in the plot) also makes clear the importance of the high-k dielectric film type and quality, since the Q of 54,158 achieved via the TiO_2-only case is still much higher than the HfO_2-only case of [8], which used an inferior ALD tool to deposit HfO_2.

It should be noted that ALD film coating does change the resonance frequency of each disk, most likely due to a combination of mass loading and an equivalent stiffness change caused by ALD film stress. Therefore, to better compare resonator Q's and peak heights for different ALD coating experiments, the data in Fig. 7 is normalized to a common frequency axis by applying to all data points the expression

$$\% f_{Norm} = \frac{f - f_o}{f_o} \times 100 \qquad (2)$$

where f_o is the center frequency of each disk and f is the measurement frequency of the data point. Table 1 provides a summary and comparison of all measured results.

Effect of Parasitic Resistance on Resonator Q

Parasitic resistance R_P can significantly degrade resonator Q when the impedance of the resonator is on the order of or lower than that of the parasite. Fig. 8 explains how various parasitic elements like interconnect traces and bond-pad contacts can modify the electrical equivalent *LCR* circuit of the resonator and load the

$$Q = \frac{\omega_O L_X}{R_X} \quad \Rightarrow \quad Q_L = \frac{\omega_O L_X}{R_X + 2R_P}$$
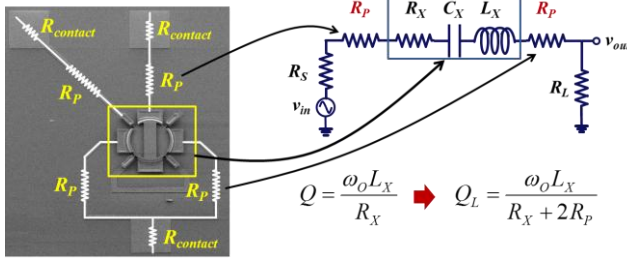
Fig. 8: (Left) SEM of the 61-MHz wineglass disk resonator used in this work. The polysilicon traces and bond-pad contacts create parasitic resistance that then load the (right) electrical equivalent LCR circuit of the resonator, lowering its Q via the indicated expression.

Table 1: Summary and comparison of measurement results for wineglass disk resonators treated with various ALD recipes.

	Before ALD	HfO$_2$ [8]	TiO$_2$	Al$_2$O$_3$ + TiO$_2$
Q	127,430	10,510	54,158	73,173
R_x	10,180 Ω	6,500 Ω	512 Ω	130 Ω
d_o	92 nm	32 nm	35 nm	37 nm
V_P	9V	5V	9V	17 V

resonator Q via the expression shown. This work uses 400 nm-thick doped polysilicon traces as interconnect, as shown in Fig. 8, for which the measured parasitic resistance is $R_P = 1.2$ kΩ. Compared to the motional resistance $R_x = 130$ Ω achieved by the Al$_2$O$_3$-TiO$_2$-coated device of this work, such a large parasitic resistance leads to a loaded Q that is 10.2x smaller than the actual Q of the device alone (without interconnects), and this is what is actually measured. Since the focus here is on the Q and R_x of the resonator device alone, sans the effect of interconnects, the data plotted in Fig. 7 represents the actual Q of each device after extracting out loading by parasitic resistance using the expression in Fig. 8.

Extraction of the gap spacing d_{gap}

As described in [8], the effective gap spacing of any capacitively transduced micromechanical resonator can be conveniently extracted by utilizing the electrical-stiffness-derived dependence of resonance frequency ω_o on the applied bias voltage V_P and the gap spacing d_{gap}. Fig. 9 presents measured curves of frequency and motional resistance vs. bias voltage for the Al$_2$O$_3$+TiO$_2$-coated resonator, all of which can be curve fitted simultaneously to reveal an effective gap spacing of 37nm; nominal zero-bias resonance frequency and Q's of 60.68 MHz and 73,173, respectively; and a motional resistance (with series interconnect resistance removed) of only 130 Ω, as advertised.

CONCLUSION

This work demonstrates the first VHF micromechanical resonators in any material, piezoelectric or not, to meet the simultaneous high Q (>50,000) and low motional resistance (<200Ω) commonly desired in many RF and frequency control applications. In doing so, it disproves to a large extent the common misconception that capacitively transduced resonators always exhibit high impedance. Interestingly, however, even as this work confirms the low impedance prowess of capacitive micromechanical resonators, other research begins to question the need for such low impedance in RF and other applications, and actually makes a case that higher impedance is preferred when a system can be fully integrated onto a single chip [18]. Whether or not low impedance is actually needed in the end, one can at least rest assured that capacitive resonators can provide it, while also simultaneously delivering Q's in the
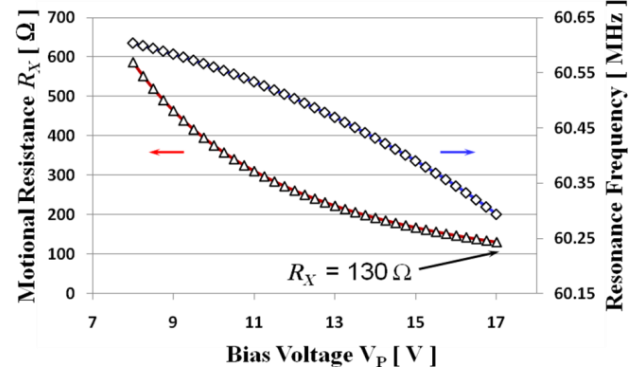

Fig. 9: Measured curves of motional resistance (bottom curve) and resonance frequency (top curve) versus dc-bias. The electrical stiffness effect observed in the latter is used to extract the effective electrode-to-resonator gap spacing of a given device [8].

tens of thousands.

REFERENCES

[1] Ruby R.C., et al., "Thin Film Bilk Wave Acoustic Resonators for Wireless…", Ultrasonic Sym., 2001 IEEE, Vol.1, pp. 813-821

[2] G. Piazza, "Integrated Aluminum Nitride Piezoelectric MEMS …", J. of Vac. Sci. Technol. A, 2009, Vol. 27, No. 4, pp 776-784

[3] Yue C.P., et al., "On-chip spiral inductors with patterned ground …", IEEE J. of Solid-State Cir., 1998, Vol.33, no 5,pp. 743-752

[4] S.-S. Li, et al., "Micromechanical Hollow-Disk…," Proceedings, 17th Int. IEEE MEMS Conf., Jan. 25-29, 2004, pp. 821-824.

[5] C. T.-C. Nguyen, "Integrated micromechanical RF…", 26th Sym. on Sensors, Micromachines & App. Sys., Tokyo, 2009, pp. 1-5.

[6] Y.-W. Lin, et al., "Series-resonant VHF micromechanical res...," IEEE J. Solid-State Cir., vol. 39, no. 12, pp. 2477-2491, 2004.

[7] S.-S. Li, et al., "Self-switching vibrating micro…", IEEE Int. Freq. Cont./Pre. T. & T. Int. Sym., Canada, 2005, pp. 135-141.

[8] Hung L.-W., et al., "Capacitive Transducer Strengthening Via ALD-Enabled Partial-Gap Filling", Hilton-Head'08.

[9] Y.-W. Lin, et al., "Third-order intermodulation distortion in capacitively…", IEEE Int. Ultrasonics Sym., 2005, pp. 1592-1595.

[10] Tiffany J. Cheng , Sunil Bhave, "High-Q, low impedance polysilicon resonators with 10nm air gaps", MEMS'10, pp. 695-698.

[11] Hung L.-W., et al., "Silicide-Based Release of High Aspect-Ratio Microstructures ", MEMS 2010, Hong Kong, pp. 120-123

[12] Y.-W. Lin, et al., "Vibrating micromechanical resonators…", IEEE Int. Freq. Cont./Prec. T. & T. Int. Sym., 2005, pp. 128-134.

[13] Markku Leskela, Mikko Ritala,"Atomic layer deposition (ALD): from precursors…", Thin Solid Films, 2002, pp.138-146.

[14] H. Cheng, et al., "Substrate Materials and Deposition Temperature Dependent…", Jou. of The Electrochem. Soc., v.156, 2009.

[15] A.C. Dillon, S.M. George, et al., "Surface chemistry of Al$_2$O$_3$ deposition using Al(CH$_3$)$_3$…", Surface Sci., vol. 322, Jan. 1995.

[16] M.D. Groner, S.M. George, et al., "Electrical characterization of thin Al$_2$O$_3$ films …", Thin Solid Films, vol. 413, Jun. 2002.

[17] M. A. Abdelmoneum, et al., "Stemless wine-glass-mode disk micromechanical reson.", MEMS'03, Kyoto, Japan, pp. 698-701.

[18] Y. Xie, et al., "UHF Micromechanical Extensional Wine-Glass Mode Ring Resonators", IEDM 2003, Washington, pp. 953-956.

CONTACT
* Mehmet Akgul, tel: +1-510-684-2166; akgul@berkeley.edu